PROCEEDINGS OF SCIENCE

SUSY searches in photonic final states with CMS

Tribeni Mishra on behalf of the CMS Collaboration[a,*]

[a] *National Institute of Science Education and Research, Jatni, Khurda, India*

E-mail: tribeni.mishra@niser.ac.in

The latest results of searches for supersymmetry in photonic final states with the CMS experiment will be presented. The analyses are based on the full dataset of proton-proton collisions collected during Run 2 of the LHC at a center-of-mass energy of 13 TeV. The results are interpreted in models including the stealth supersymmetry models and gauge-mediated supersymmetry breaking models.

The European Physical Society Conference on High Energy Physics (EPS-HEP2023)
21-25 August 2023
Hamburg, Germany

*Speaker

https://pos.sissa.it/

PoS(EPS-HEP2023)454

1. Introduction

Supersymmetry (SUSY) [1] stands as a crucial extension of the standard model (SM), addressing unresolved issues within it. In scenarios involving gauge-mediated supersymmetry breaking (GMSB) [2], pairs of colored SUSY particles such as gluinos ($\tilde{g}$), squarks ($\tilde{q}$), or gauginos ($\tilde{\chi}^0$, $\tilde{\chi}^\pm$) are generated. The lightest SUSY particle (LSP) [3], typically the gravitino ($\tilde{G}$), remains stable, causing missing transverse momentum ($p_\mathrm{T}^\mathrm{miss}$) in the event. The next-to-lightest supersymmetric particle (NLSP), e.g., neutralinos ($\tilde{\chi}^0$), charginos ($\tilde{\chi}^\pm$), sleptons ($\tilde{\ell}$), or squarks, decays into SM particles and gravitino. When the neutralino NLSP is predominantly bino-like, its primary decay mode includes a $\tilde{G}$ and a photon (γ), leading to final states characterized by $p_\mathrm{T}^\mathrm{miss}$ and one or more photons.

As searches at LHC using high $p_\mathrm{T}^\mathrm{miss}$ events set ever more stringent lower bounds on stop ($\tilde{t}$) masses, searches for low $p_\mathrm{T}^\mathrm{miss}$ alternatives become increasingly crucial. A specific model, known as the stealth scenario [4], introduces a light-hidden sector to the SUSY model. The CMS [5] detector efficiently reconstructs and identifies photons with high accuracy, crucial in mitigating SM backgrounds. Additionally, in GMSB models, the presence of photons is particularly significant, enhancing sensitivity to such models. This report discusses three CMS analyses, two [6, 7] targeting GMSB models and one [8] exploring the low $p_\mathrm{T}^\mathrm{miss}$ signature in the stealth SUSY scenario.

1.1 SUSY search in events with a photon, a lepton and $p_\mathrm{T}^\mathrm{miss}$ using 2016 data

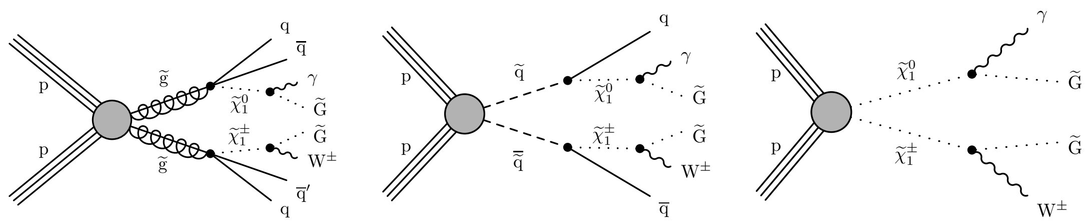

Figure 1: Diagrams showing gluino ($\tilde{g}$) pair production with $\tilde{g} \to q\bar{q}\tilde{\chi}_1^0/\tilde{\chi}_1^\pm$(left), squark ($\tilde{q}$) pair production with $\tilde{q} \to q\tilde{\chi}_1^0/\tilde{\chi}_1^\pm$ (center), and direct production of neutralino-chargino pair (right) [6]

In this analysis [6], the results of a search for SUSY in events with one photon γ, at least one lepton ℓ (electron or muon), and significant $p_\mathrm{T}^\mathrm{miss}$ are presented. The data sample corresponds to an integrated luminosity of 35.9 fb^{-1} of proton-proton (pp) collision data at a center-of-mass energy of 13 TeV, collected by the CMS detector in 2016. The analysis focuses on three simplified models depicted in Fig. 1: gluino pair production, squark pair production, and direct production of a neutralino-chargino pair. It is performed in both the $e\gamma$ and $\mu\gamma$ channels. The $e\gamma$ data sample is collected using a diphoton trigger requiring specific p_T thresholds and invariant mass criteria for the electromagnetic objects. In the $\mu\gamma$ channel, events are collected using two muon-photon cross-triggers requiring specific p_T thresholds for muons and photons. Candidate signal events are required to contain at least one isolated photon with $\mathrm{p_T} > 35$ GeV and $|\eta| < 1.44$ and at least one isolated electron (muon) with $p_\mathrm{T} > 25$ GeV and $|\eta| < 2.5$ (2.4). In the $e\gamma$ channel, the $e\gamma$ invariant mass must exceed the Z boson mass by 10 GeV to reduce misidentification. The signal region (SR) is defined as $p_\mathrm{T}^\mathrm{miss} > 120$ GeV and $\mathrm{m_T} > 100$ GeV, where $\mathrm{m_T}$ is the transverse mass of the

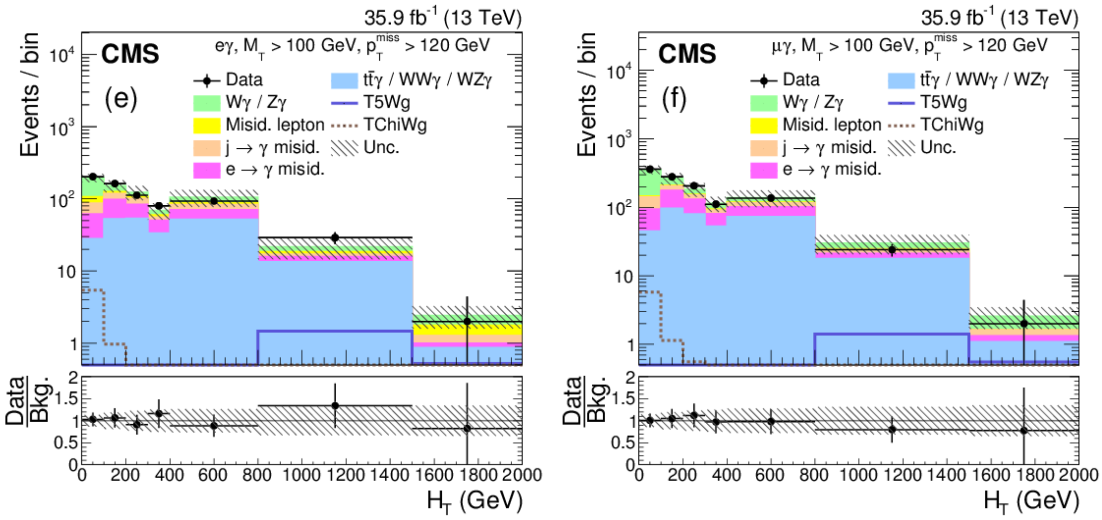

Figure 2: Distributions of H_T from data (points) and estimated SM predictions (stacked histograms) for the $e\gamma$ (left) and $\mu\gamma$ (right) channels, overlaid with two signal distributions [6]

lepton and p_T^{miss} system. The SR is further divided into bins based on p_T^{miss}, photon p_T, and H_T, the scalar sum of the p_T of all jets that are separated from both the candidate photon and candidate lepton. Several SM processes can produce similar signatures as the targeted SUSY signal and are called SM backgrounds. The main background is the production of a W or Z boson in association with a photon (V + γ). In particular, the neutrinos from leptonic W decays escape the detector and result in genuine p_T^{miss}. The second category contains misidentified objects, including fake photons from mis-reconstructed electrons or jets and fake leptons from non-prompt productions. Such backgrounds are derived from data-driven methods in $p_T^{miss} < 70$ GeV control regions (CRs), which are non-overlapping with the baseline selection and extrapolated into the SR. The rare backgrounds are associated productions of multiboson or top quarks with a photon, estimated using simulation. Figure 2 illustrates the agreement between observed data and predicted backgrounds in the SR, considering the systematic uncertainties. These results are interpreted in the context of the upper

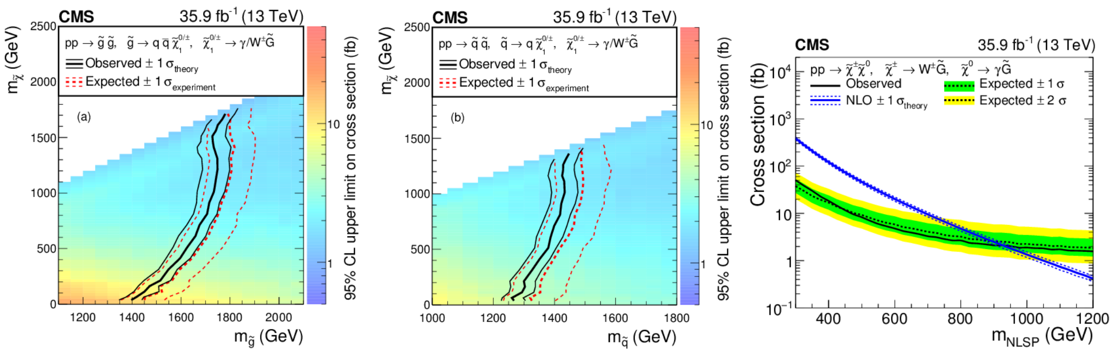

Figure 3: Expected and observed limits in the $m_{\tilde{g}}$ versus $m_{\tilde{\chi}}$ mass plane are presented for the $\tilde{g} \to q\bar{q}\tilde{\chi}_1^0/\tilde{\chi}_1^{\pm}$ model (left), as well as in the $m_{\tilde{q}}$ versus $m_{\tilde{\chi}}$ mass plane for the $\tilde{q} \to q\tilde{\chi}_1^0/\tilde{\chi}_1^{\pm}$ model (middle). Limits on the $\tilde{\chi}_1^0\tilde{\chi}_1^{\pm}$ pair production cross section, as a function of the NLSP ($\tilde{\chi}_1^0$, $\tilde{\chi}_1^{\pm}$) mass is shown (right) [6]

limit on the cross sections of the three simplified SUSY models targeted in this analysis. Gluino masses up to 1.75 TeV and squark masses up to 1.43 TeV are excluded at 95% confidence level (CL) for gluino and squark pair production models, respectively, as shown in Fig. 3. Additionally, the electroweak production model excludes gaugino masses below 930 GeV, as demonstrated in Fig. 3.

1.2 SUSY search in events with photons, jets and $p_{\mathrm{T}}^{\mathrm{miss}}$ using Run 2 data

This paper [7] explores signatures of SUSY particles produced via strong and electroweak interactions using 137 fb^{-1} pp collision data collected by CMS from 2016 to 2018. It focuses on final states with at least one photon, multiple jets, and significant $p_{\mathrm{T}}^{\mathrm{miss}}$. If the NLSP is a $\tilde{\chi}_1^{\pm}(\tilde{\chi}_1^0)$, its decay results in a W (γ, or Z, or Higgs) boson and a $\tilde{G}$. Representative diagrams for gluino and stop pair production are shown in Fig. 4. Diagrams illustrating $\tilde{\chi}^{\pm}\tilde{\chi}^0$ and $\tilde{\chi}^{\pm}\tilde{\chi}^{\pm}$ pair production can be

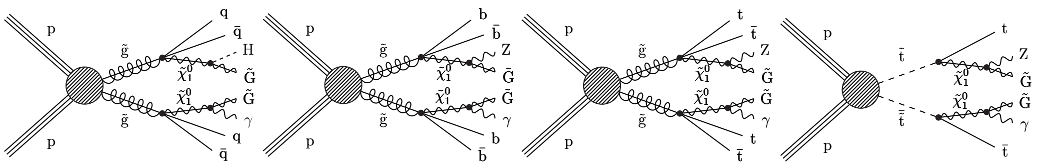

Figure 4: Diagrams depicting $\tilde{\mathrm{g}}\tilde{\mathrm{g}}$ pair production with : (left) $\tilde{\mathrm{g}} \to \mathrm{q}\bar{\mathrm{q}}\tilde{\chi}_1^0$ followed by $\tilde{\chi}_1^0 \to \widetilde{\mathrm{G}}\mathrm{H}/\gamma$, (middle-left) $\tilde{\mathrm{g}} \to \mathrm{b}\bar{\mathrm{b}}\tilde{\chi}_1^0$ followed by $\tilde{\chi}_1^0 \to \widetilde{\mathrm{G}}\mathrm{Z}/\gamma$, (middle-right) $\tilde{\mathrm{g}} \to \mathrm{t}\bar{\mathrm{t}}\tilde{\chi}_1^0$ followed by $\tilde{\chi}_1^0 \to \widetilde{\mathrm{G}}\mathrm{Z}/\gamma$, (right) $\tilde{\mathrm{t}}\bar{\tilde{\mathrm{t}}}$ pair production with $\tilde{\mathrm{t}} \to \mathrm{t}\tilde{\chi}_1^0$ followed by $\tilde{\chi}_1^0 \to \widetilde{\mathrm{G}}\mathrm{Z}/\gamma$ [7]

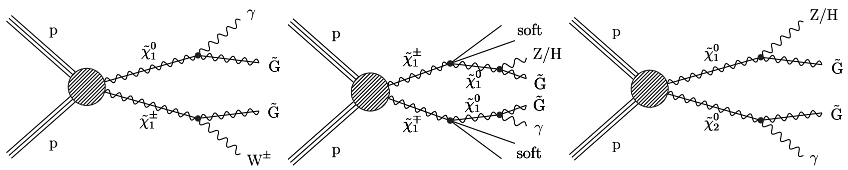

Figure 5: Diagrams showing the production of $\tilde{\chi}_1^{\pm}\tilde{\chi}_1^0$ (left) and $\tilde{\chi}_1^{\pm}\tilde{\chi}_1^{\pm}$ (middle), and $\tilde{\chi}_1^0\tilde{\chi}_2^0$ (right) [7]

found in Fig. 5. In both scenarios, the masses of charginos and neutralinos are degenerate. The SRs for electroweakino searches are reoptimized, incorporating jets consistent with hadronic decays of W, Z, or Higgs bosons. Events are required to have $p_{\mathrm{T}}^{\mathrm{miss}} > 300$ GeV, $\mathrm{N_{jets}}$ (number of jets) ≥ 2, and at least one photon with $\mathrm{p_T} > 100$ GeV and $|\eta| < 2.4$, separated from jets by $\triangle R(\mathrm{jet}, \gamma) > 0.3$. The scalar p_{T} sum of jets and photons ($\mathrm{S_T}$) must exceed 300 GeV. Additionally, events with isolated leptonic or hadronic tracks are rejected, eliminating 40% of relevant SM background processes. The SRs are defined based on $p_{\mathrm{T}}^{\mathrm{miss}}$, presence of vector boson (V-tag) or Higgs boson (H-tag), $\mathrm{N_{jets}}$, and $\mathrm{N_{b-tags}}$ (number of b-tagged jets).

The SM backgrounds for this search can be classified into four categories. Events like $W\gamma$+jets and $tt\gamma$+jets, with a prompt photon and a W boson decay to $\ell'\nu$ (ℓ' = e, μ, or τ leptons), contribute to the "lost-lepton background" if the e or μ leptons remain unidentified or if the τ leptons decay hadronically ("hadronic τ"). To estimate this background, a control sample of $e(\mu) + \gamma$ events is scaled using a simulation-based transfer factor. Another SM background arises from W boson production, where $W \to e\bar{\nu}$ and the electron is misidentified as a photon. This background is estimated using a control sample of single electrons, scaled by the fake rate representing the probability of electrons being misidentified as photons. Additionally, the irreducible background

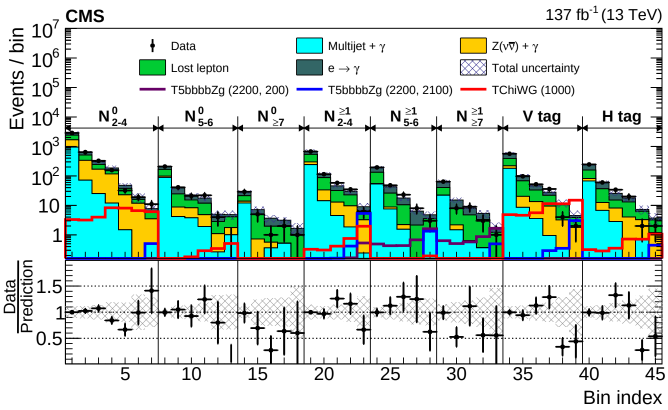

Figure 6: Predicted background events displayed as stacked histograms, with observed events depicted as black points in SRs and low-p_T^{miss} CRs [7]

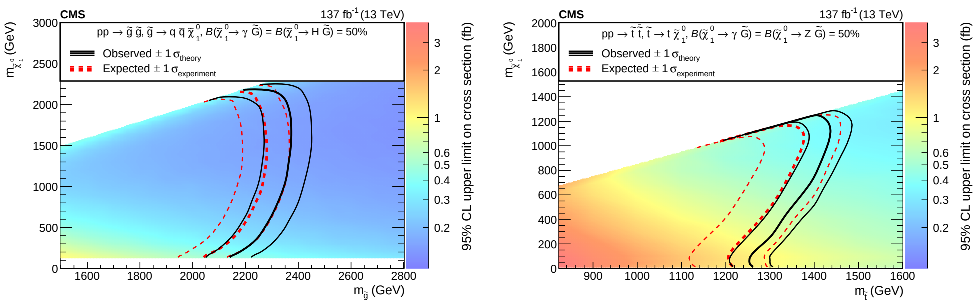

Figure 7: Expected and observed limits in the $m_{\tilde{g}}$ versus $m_{\tilde{\chi}_1^0}$ mass plane are presented for the $\tilde{g} \to q\bar{q}\tilde{\chi}_1^0$ model (left), as well as in the $m_{\tilde{t}}$ versus $m_{\tilde{\chi}_1^0}$ mass plane for the $\tilde{t} \to t\tilde{\chi}_1^0$ model (right) [7]

comes from the $Z(\to \nu\bar{\nu}) + \gamma$ process. To estimate this background, $Z(\to \nu\bar{\nu}) + \gamma$ simulation is scaled by the yield of $Z(\to \ell\bar{\ell}) + \gamma$ events in data, accounting for branching ratios. Furthermore, mismeasurements in p_T of one or more jets in γ+jets and QCD events can result in large p_T^{miss} in reconstructed events. To predict this jet mismeasurement, the ABCD method [7] is employed, utilizing low p_T^{miss} and $\Delta\phi$ (p_T^{miss}, jet) sidebands. As illustrated in Fig. 6, observed event yields in most SRs align closely with the SM predictions, indicating no significant signal events. The results are interpreted in the context of the upper limit on the cross sections of various SUSY models. Figure 7 (left) presents the lower limit for gluino mass, reaching 2.35 TeV in models where $\tilde{g} \to q\bar{q}\tilde{\chi}_1^0$ and $\tilde{\chi}_1^0 \to$H$\widetilde{G}$ or $\gamma\widetilde{G}$ with equal probability. Similarly, the right panel of Fig. 7 shows a top squark mass limit of 1.43 TeV in models with $\tilde{t} \to t\tilde{\chi}_1^0$ and subsequent decays $\tilde{\chi}_1^0 \to$ Z $\widetilde{G}$. Figure 8 (left) illustrates the exclusion of chargino and neutralino masses up to 1.23 TeV, considering wino-like electroweakinos decaying into $\tilde{\chi}_1^{\pm} \to$W$\widetilde{G}$ and $\tilde{\chi}_1^0 \to \gamma\widetilde{G}$. Additionally, Fig. 8 (middle) shows higgsino-like electroweakino mass limits reaching 1.05 TeV in models where $\tilde{\chi}_1^0 \to \gamma\widetilde{G}, Z\widetilde{G}, H\widetilde{G}$ with branching fractions of 50%, 25%, and 25%, respectively. In a model involving only $\tilde{\chi}_1^0\tilde{\chi}_2^0$ process, the observed NLSP mass limit is 0.5 TeV, as displayed in Fig. 8 (right).

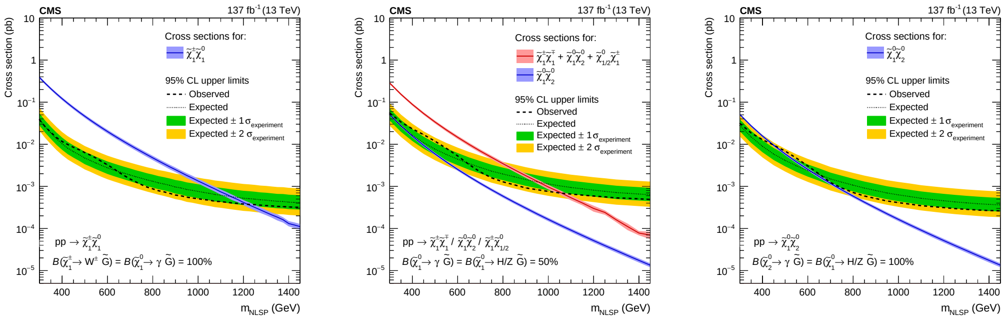

Figure 8: Expected and observed limits on the cross-section of $\tilde{\chi}^0_1\tilde{\chi}^\pm_1$ pair production (left), combined ($\tilde{\chi}^\pm_1\tilde{\chi}^\mp_1$ + $\tilde{\chi}^0_1\tilde{\chi}^0_2$ + $\tilde{\chi}^0_1\tilde{\chi}^\pm_1$ + $\tilde{\chi}^0_2\tilde{\chi}^\pm_1$) process (middle) and $\tilde{\chi}^0_1\tilde{\chi}^0_2$ process only (right), as a function of the NLSP masses [7]

1.3 SUSY search in events with diphotons, jets and low $p_{\mathrm{T}}^{\mathrm{miss}}$ using Run 2 data

Stealth SUSY models featuring the pair production of squarks or gluinos are focused in this study [8], as illustrated in Fig. 9. The dataset corresponds to 138 fb^{-1} of pp collision data at a center-of-mass energy of 13 TeV, collected by the CMS detector from 2016 to 2018. In these models, a hidden sector is introduced, comprising a single scalar boson, denoted as a singlet S, and its corresponding SUSY fermion, the singlino $\widetilde{S}$. The colored SUSY particles decay to neutralinos by emitting quarks. These neutralinos decay to singlinos through photon emission, and the singlinos subsequently decay into singlets and gravitinos, as the LSP. The singlet and singlino have almost identical masses, leading to a distinct low $p_{\mathrm{T}}^{\mathrm{miss}}$ signature in the final state. Thus, the final state consists of two photons, many jets, and low $p_{\mathrm{T}}^{\mathrm{miss}}$ carried by the light, soft gravitinos.

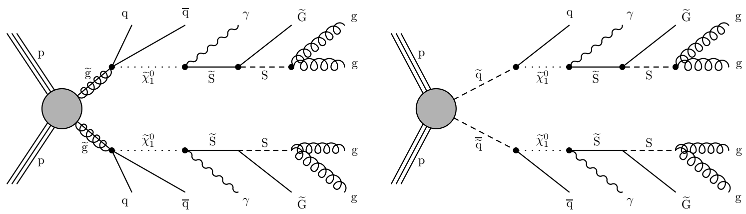

Figure 9: Diagrams for production of either gluino pairs (left) or squark pairs (right), and results in a final state consisting of two photons, multiple jets, and low $p_{\mathrm{T}}^{\mathrm{miss}}$

Events with $\mathrm{S_T} > 1200$ GeV and at least two reconstructed jets are considered for this analysis, where $\mathrm{S_T}$ is the scalar p_{T} sum of jets, photons, and $p_{\mathrm{T}}^{\mathrm{miss}}$ in the event. The jets are required to have a minimum ΔR separation of 0.4 from a photon. The analysis employs diphoton triggers, which require two photons with leading and subleading p_{T} thresholds of 30 GeV and 18 GeV, respectively, and require a 55 GeV invariant mass for the two photons. The SR includes events with four or more jets and $\mathrm{S_T} > 1300$ GeV and is divided into three $\mathrm{N_{jets}}$ bins (4, 5, and ≥ 6) and six $\mathrm{S_T}$ ranges (1300–1400, 1400–1500, 1500–1700, 1700–2000, 2000–2500, and > 2500 GeV), resulting in 18 distinct SRs. The primary background in this search comes from multijet events with two photons originating from the initial scattering. Specifically, multijet backgrounds with high $\mathrm{N_{jets}}$ can be determined using the $\mathrm{S_T}$ shape invariance method. The central concept is that the $\mathrm{S_T}$ distribution

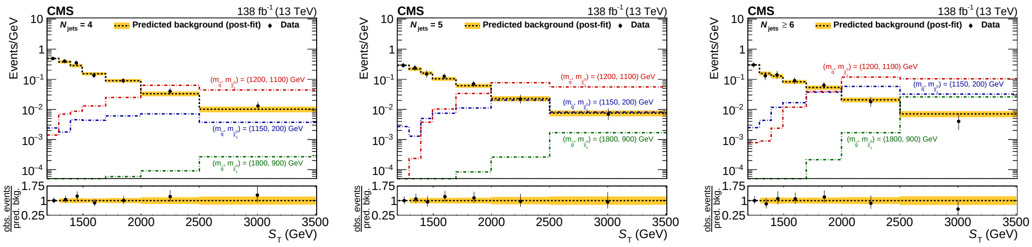

Figure 10: Comparison of the measured S_T distribution with the post-fit background prediction for N_{jets} = 4 (left), 5 (center), and ≥6 (right), showing post-fit uncertainties as yellow band [8]

in events with low N_{jets} values, where signal contamination is minimal for the studied models, can be extrapolated to predict the background S_T distribution at high N_{jets}. The comparison between

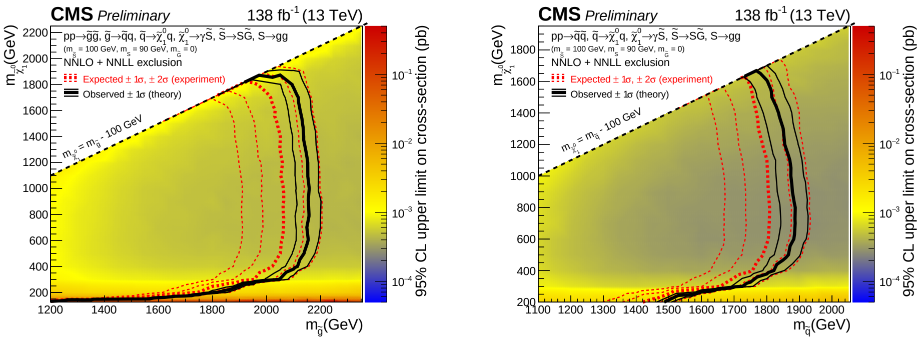

Figure 11: Expected and observed limits on gluino pair production cross-section (left) and squark pair production cross-section (right) as a function of gluino (squark) and neutralino masses [8]

the measured S_T distribution and the post-fit background prediction, considering uncertainties, is illustrated in Fig. 10 for various jet multiplicities. The data reveal no indication of any deviation from the background prediction. These results are interpreted as 95% CL upper limits on the cross-sections for gluino and squark pair production in simplified stealth SUSY models. Figure 11 illustrates these upper limits as a function of gluino (squark) and neutralino masses. For most neutralino masses, gluino masses up to 2150 GeV and squark masses up to 1850 GeV are excluded at a 95% CL.

2. Summary

Three analyses [6–8] focusing on final states with photons are presented. The analysis [7], involving photons, jets, and p_T^{miss} achieves enhanced sensitivity to scenarios with small mass differences between gluinos and NLSP. The search strategy is expanded to provide sensitivity to the production of electroweakino pairs, establishing the most stringent limits on electroweakino production with photons in the final state. In the stealth SUSY analysis [8], a significant ~70% improvement in the exclusion contour in the $(m_{\tilde{q}}, m_{\tilde{\chi}^0})$ parameter space is achieved. These analyses utilize the accurate photon reconstruction capabilities of the CMS detector, increasing the sensitivity for GMSB models and deepening our insights into stealth SUSY.

References

[1] S. P. Martin, "A Supersymmetry Primer", arXiv:hep-ph/9709356

[2] E. Poppitz and S.P. Trivedi, "Some remarks on gauge mediated supersymmetry breaking", Phys. Lett. **B 401**, 38 (1997)

[3] G. R. Farrar and P. Fayet, "Phenomenology of the production, decay, and detection of new hadronic states associated with supersymmetry", Phys. Lett. **B 76**, 575 (1978)

[4] J. Fan, M. Reece, and J. T. Ruderman, "Stealth supersymmetry", JHEP **11**, 012 (2011)

[5] CMS Collaboration, "The CMS experiment at the CERN LHC", JINST **3**, S08004 (2008)

[6] CMS Collaboration, "Search for supersymmetry in events with a photon, a lepton, and missing transverse momentum in proton-proton collisions at $\sqrt{s}$= 13 TeV", JHEP **01**, 154 (2019)

[7] CMS Collaboration, "Search for new physics in multijet events with at least one photon and large missing transverse momentum in proton-proton collisions at 13 TeV", JHEP **10**, 046 (2023)

[8] CMS Collaboration, "Search for stealth SUSY in final states with two photons, jets, and low missing transverse momentum", arXiv:2310.03154